U.S. Navy Journal of Underwater Acoustics Volume 64, Issue 4 JUA_2015_026_L
October 2014

INTERNAL WAVE IMPACT ON THE PERFORMANCE OF A HYPOTHETICAL MINE HUNTING SONAR

Stewart M. Simpson and Edward J. Tucholski
Physics Department
U.S. Naval Academy
Annapolis, MD 21402

Marshall H. Orr
The University of Delaware
The College of Earth, Ocean, and Environment
Newark, DE 19716

(Received February 19, 2015)

Acoustic signals exhibit continuous spatial and temporal variability when propagating through a sound speed field that is perturbed by oceanic internal waves. Consequently, acoustic systems operating in an internal wave perturbed sound speed field will exhibit performance variability. Numerical simulations are presented which quantify the impact of oceanic internal waves on the performance of a hypothetical mine hunting sonar system operating near a continental shelf break. They show the signal excess (probability of target detection) of a mine hunting sonar system will be temporally and spatially variable and dependent on: 1. the figure of merit parameters selected for the system's operation, 2. the sonar projector depth, and 3. the target depth and range.

I. INTRODUCTION

Mine hunting sonar systems may be operated on continental shelves in sound speed fields that are perturbed by a variety of fluid dynamic processes including propagating internal wave groups.[1] The development of optimal deployment and search strategies for systems operating in such environments requires a quantitative understanding of their performance variability. Calculations have been performed to quantify the performance variability of a mine hunting sonar projecting signals parallel to the propagation vector of an internal wave group generated near a continental shelf break.

A range dependent sound speed field was synthesized from experimental data acquired in the early fall of 2000 on the New Jersey USA shelf during the NRL/ONR Shallow Water Acoustic Technology (SWAT) experiment. The resulting 4.5 km long internal wave perturbed sound speed field was moved in discrete steps through a mine field that was being observed with a hypothetical mine hunting sonar system operating in backscatter mode using a 20 kHz source placed at a fixed depth within the water column. The time dependent variability of acoustic signal incident on each target in the mine field was calculated for two selected acoustic source depths, one above and one below the seasonal thermocline. The targets were placed at a number of ranges and depths within the water column and on the ocean bottom. The Navy Standard Comprehensive Acoustic System Simulation/Gaussian Ray Bundle (CASS/GRAB) computer program[2,3] was

Table of Contents

Report Documentation Page

Form Approved
OMB No. 0704-0188

1. REPORT DATE	2. REPORT TYPE	3. DATES COVERED
OCT 2014	**N/A**	**-**

4. TITLE AND SUBTITLE	5a. CONTRACT NUMBER
Internal Wave Impact on the Performance of a Hypothetical Mine Hunting Sonar (U)	5b. GRANT NUMBER
	5c. PROGRAM ELEMENT NUMBER
6. AUTHOR(S)	5d. PROJECT NUMBER
	5e. TASK NUMBER
	5f. WORK UNIT NUMBER
7. PERFORMING ORGANIZATION NAME(S) AND ADDRESS(ES) **U.S. Naval Academy Annapolis, MD 21402**	8. PERFORMING ORGANIZATION REPORT NUMBER
9. SPONSORING/MONITORING AGENCY NAME(S) AND ADDRESS(ES)	10. SPONSOR/MONITOR'S ACRONYM(S)
	11. SPONSOR/MONITOR'S REPORT NUMBER(S)

12. DISTRIBUTION/AVAILABILITY STATEMENT
Approved for public release, distribution unlimited

13. SUPPLEMENTARY NOTES
See also ADC084441. U.S. Navy Journal of Underwater Acoustics. Volume 64, Issue 4, October 2014 - General Issue, The original document contains color images.

14. ABSTRACT

15. SUBJECT TERMS

16. SECURITY CLASSIFICATION OF:			17. LIMITATION OF ABSTRACT	18. NUMBER OF PAGES	19a. NAME OF RESPONSIBLE PERSON
a. REPORT	b. ABSTRACT	c. THIS PAGE			
unclassified	**unclassified**	**unclassified**	**SAR**	**15**	

Standard Form 298 (Rev. 8-98)
Prescribed by ANSI Std Z39-18

used to calculate the variability of the intensity of the acoustic signal incident on each target and the acoustic field transmission loss variability.

By estimating the magnitude of acoustic signal scattered from the targets and received by the mine hunting sonar, signal excess (*SE*) variability was calculated for a defined system figure of merit (*FOM*).

II. SOUND SPEED FIELD GENERATION

Conductivity and temperature versus depth (CTD) data acquired on the New Jersey Shelf from October 3, 2000, 22:28:28 Z, to October 4, 2000, 1:57:08 Z, was used to generate a range dependent sound speed field. The data was taken as several mode one internal waves passed beneath a research vessel, (R/V) *Endeavor*, which was moored in ~ 68 m deep water at the location shown in Fig. 1.[4] The CTD instrument package was raised and lowered vertically through the water column with a winch. Twenty consecutive CTD casts taken during a ~ 200-minute time interval were used to construct a sound speed field. Each CTD cast generated two independent sound velocity profiles, one on the down cast and one on the up cast, for a total of 40 independent profiles. The sound speed field was composed of two nearly constant sound speed layers separated by a strong sound speed gradient near mid water depth as shown in Fig. 2.

Fig. 1 – Location of R/V *Endeavor*[4] during moored CTD operations (Lat: 39.34˚, Long: −72.88˚)

During the CTD data acquisition period, a downward looking 200 kHz high frequency acoustic backscattering sonar imaged the water column using acoustic signals scattered from neutrally buoyant acoustic impedance variability (particles, temperature and salinity gradients, and velocity fluctuations). The sonar imaged mode one internal wave vertical displacement of the neutrally buoyant scatterers as the internal waves propagated through the water column beneath the research vessel as shown in Fig. 3. The V-like structure in Fig. 3 is caused by acoustic signal backscattering from the CTD sensor package as it was lowered and raised through the water column. It is clear from the acoustic image that the CTD sampling of the water column was temporally aliased.

The vertical displacement of the acoustic scattering layers by the passing internal wave field was correlated to the temporal displacement of the sound speed field measured by the CTD. The CTD and acoustic data taken during the 200-minute time interval was converted to a range dependent sound speed field by "merging" the CTD and acoustic backscatter data sets and then converting the time record of the internal wave displacement of the sound speed field to a space record by multiplying the time by the internal wave propagation speed of 0.4 m/s. A 4.5 km long internal wave perturbed sound speed field was generated from the 40 time separated sound speed profiles.

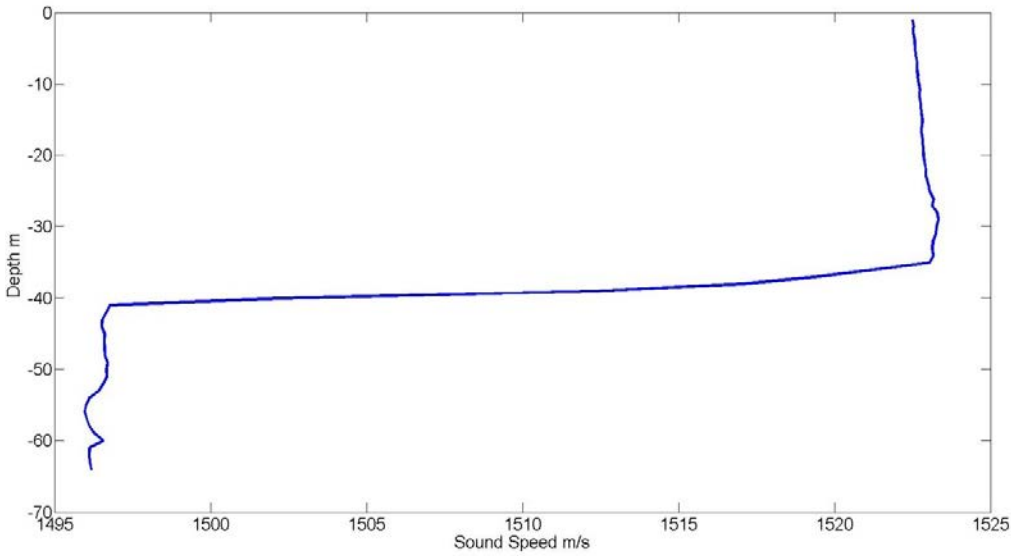

Fig. 2 – Sample sound velocity profile, X-axis (m/s), Y-axis (m)

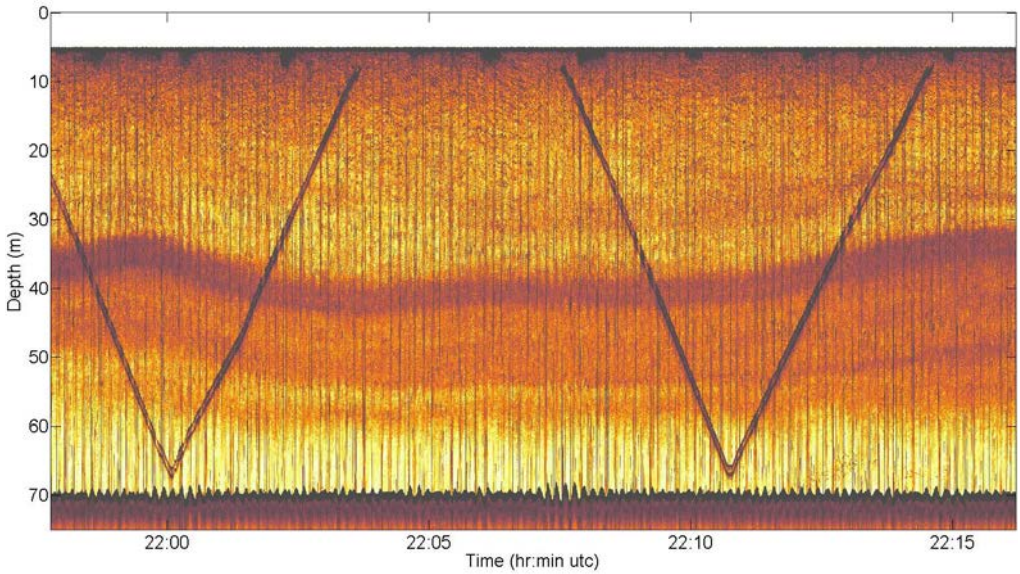

Fig. 3 – Acoustic backscatter image of a mode 1 internal wave displacement of the pycnocline. The Y-axis is depth (5–70 m), and the X-axis is time. The length of the record is about 20 minutes.

In detail, each up and down segment of a CTD cast, although distributed in time, was treated as though it was acquired instantaneously at a specific time point. The down segment of the cast was assigned a time point about half way between the start of cast and the termination of the cast. The up segment was assigned a time point at the termination of the cast. Separately, a software package (Triton Elics International Inc. Isis Sonar) was used to digitize selected acoustical scattering layers in five-second steps to obtain the scattering layer depth dependence as a function of time. The acoustic scattering layer was correlated with a sound speed by noting when the CTD down or up cast crossed the scattering layer depth. The two data sets were then merged when the sound speed correlated with the acoustic scattering layer was plotted between the down and up segment of each CTD casts. The process resulted in a continuously varying range and depth dependent sound speed profile. A 1 km section of the generated sound speed profile is displayed in Fig. 4.

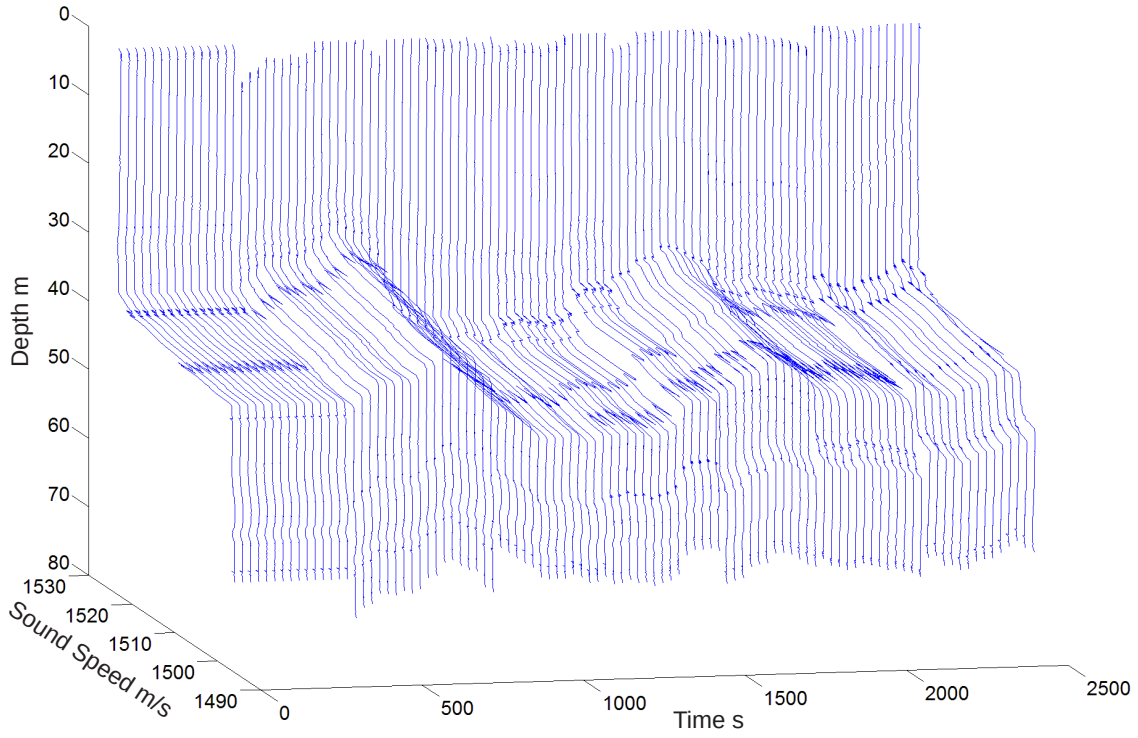

Fig. 4 – Example of generated range-dependent profile; X-axis (m/s), Y-axis (s), Z-axis (m)

III. ACOUSTIC SIGNAL PROPAGATION SIMULATION

The U.S. Navy CASS/GRAB ray trace acoustic propagation code was used to calculate the performance of a hypothetical mine hunting sonar system operating in an internal wave perturbed sound speed field. The mine hunting sonar source was placed at a fixed location and depth at the beginning of the 4.5 km sound speed field. The system performance was quantified for two deployment depths, i.e. 20 and 50 meters. The 20 kHz sonar system pinged every 25 seconds. The transducer beam pattern was a fan directed 15 degrees up and 5 degrees down from the horizontal. A MatLab script executed the CASS/GRAB software package. Spherical targets were placed at 100, 200, 400, and 800 m from the acoustic signal source and at 25, 35, 45, 60, and 70 depths as shown by the stars in Fig. 5 a and b. Acoustic signals were propagated from the mine hunting system to a range of 1000 m. The acoustic signal strength and transmission loss at each of the target was extracted. The sound speed field was then moved to the left by 10 m (25 sec time steps) to simulate the propagation of the internal wave field through the mine field. Again the transmission loss and acoustic signal strength were extracted and stored. These calculations were repeated 200 times. The CASS/GRAB calculations environmental input parameters were set for a calm surface with a wind speed of two meters per second and a flat sandy bottom.

The transmission loss to each of the targets changed as the sound speed profile moved through the mine field; see Fig. 5 a and b for a representative transmission loss calculation for the two mine hunting sonar operation depths, one above and one below the thermocline. A movie of the temporal variability of the acoustic field can be accessed from the Naval Research Laboratory.[5]

a.

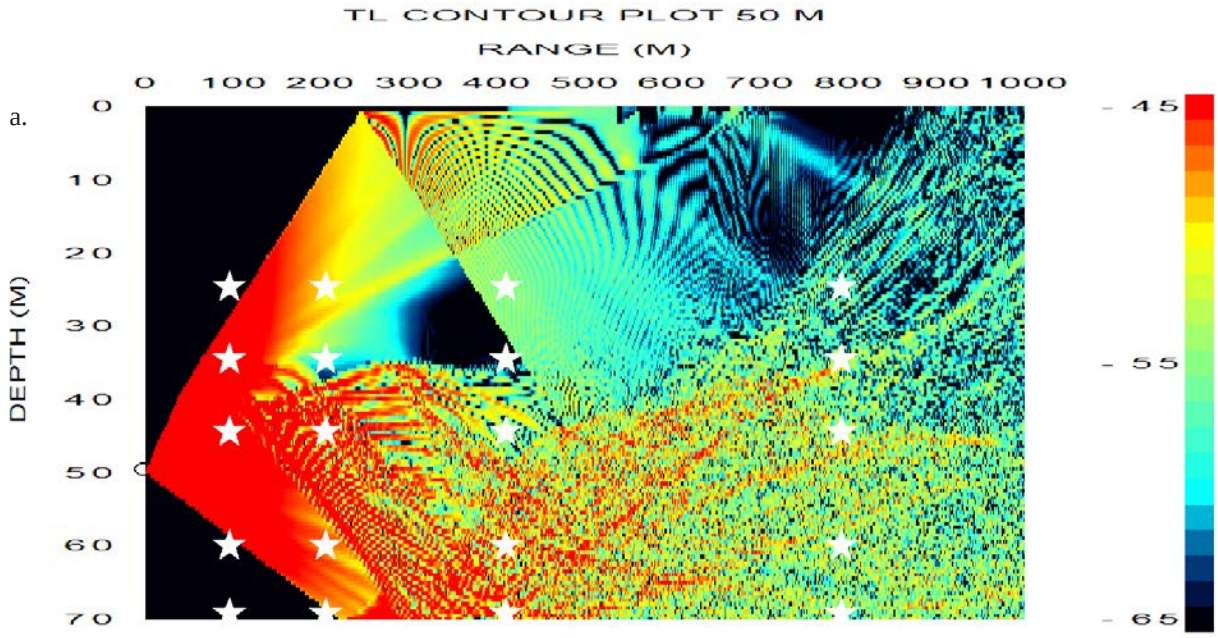

b.

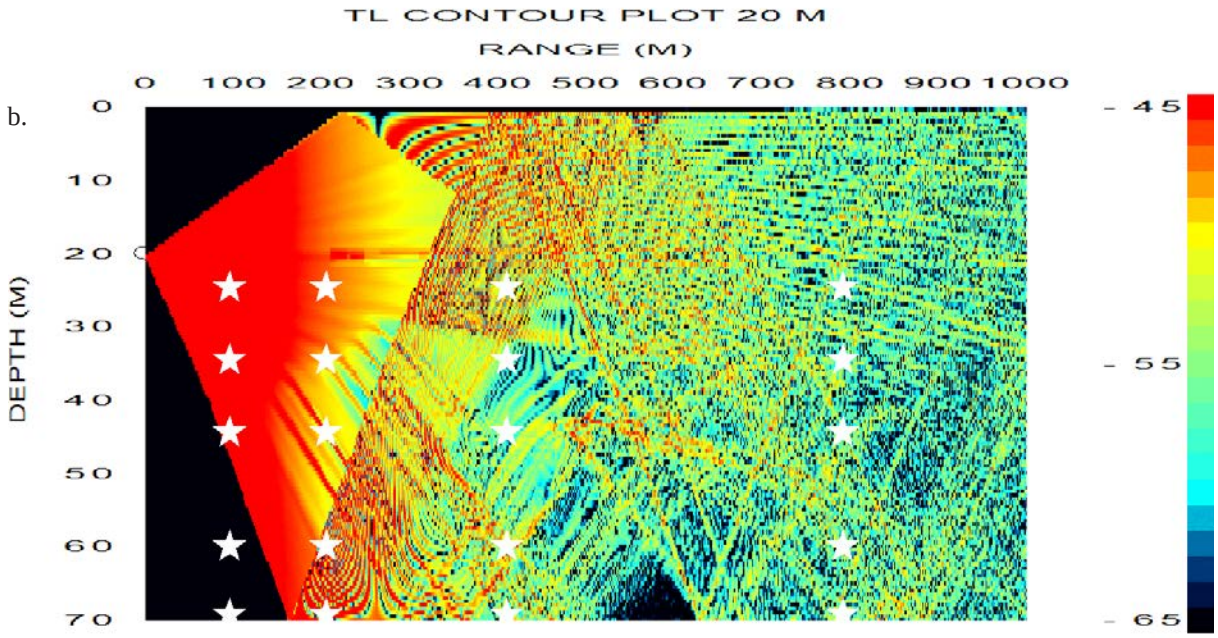

Fig. 5 – a. A contour transmission loss plot for a 20 kHz projector placed at 50 m. b. Projector placed at 20 m. Target depth is noted by the white stars. The color scale is in decibels.

IV. THE MINE HUNTING SONAR PERFORMANCE

The temporal variability of the performance of a mine hunting sonar system operating in a range and time dependent internal wave perturbed sound speed profile was evaluated by calculating the temporal variability of the signal excess (*SE*) of acoustic signals back scattered from targets distributed through the water column and on the bottom.

The *SE* was defined as the difference between the sonar system's figure of merit (*FOM*) and two times the one-way transmission loss (*TL*). It was expressed as:

$$SE = FOM - 2TL. \tag{1}$$

The calculation assumed the ocean is static during each ping's propagation time to target and back to the receiving hydrophone.

The *FOM* was defined as:

$$FOM = SL + TS - DT - NL + DI. \tag{2}$$

As an illustration, for a *SL* = Source Level = 240 dB re 1 μPa @ 1 m; *TS* = Target Strength = −6 dB; *DT* = Detection Threshold = 20 dB; *NL* = Noise Level = 58 dB, and *DI* = Directivity Index = 18 dB the *FOM* was 174 dB. The reverberation noise level is of the same magnitude as that measured at 20 kHz during ~ 10 m/s wind events. Note the CASS/GRAB calculation was done for a wind speed of ~ 1 m/s.

The variability of the *FOM* and *SE* as a function of source level is plotted in Fig. 6. The *SE* has been plotted for a *TL* of 55 and 65 dB.

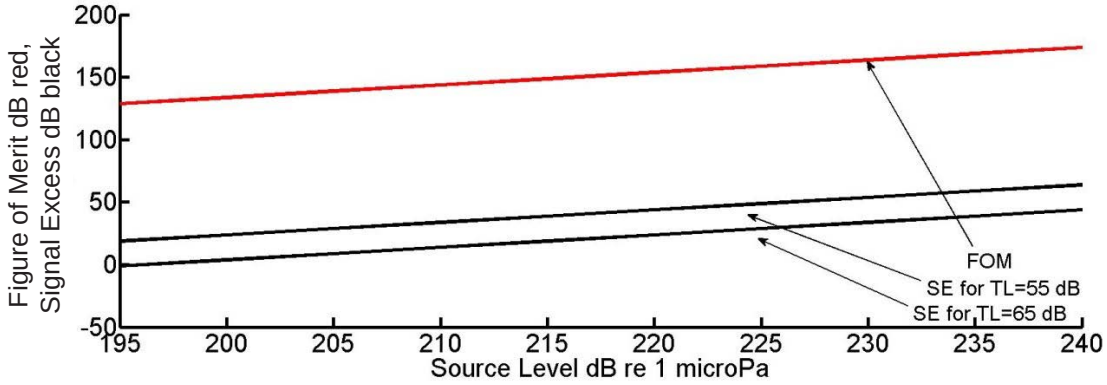

Fig. 6 – Figure of merit (red) for the parameters listed in the text. Signal excess (black) for a transmission loss of 55 (upper curve) and 65 dB (lower curve) are plotted as a function of source level.

V. RESULTS

The *SE* variability versus time caused by the internal wave perturbation of the sound speed field is plotted on the left of the Figs. 7–11 for a source depth of 50 m and spherical targets placed at 25, 35, 45, 60, and 70 m depths at ranges of 100, 200, 400, and 800 m from the sonar system. Note the targets at 70 m were on the bottom. Only *SE* greater than zero were plotted. A histogram of the *SE* variability distribution is plotted in the right column. The histogram is the probability distribution of the mine hunting sonars performance variability. The distribution was not fitted to an analytic probability

distribution because of the range and depth variability seen in the figures and the limited temporal extent of the internal wave perturbed sound field used in the simulations.

The *SE* for the target at 25 m depth shows only a few detections with *SE* => 0 at a range of 100 m and nearly continuous detections with *SE* => 0 at the 200, 400, and 800 m range points as seen in Fig. 7. Comparing both the *SE* variability versus time and the histogram of the *SE* variability shows that the magnitude or breadth of the variability increases with increasing range for the target at 25 m depth. The *TL* plot for one time instance in Fig. 5 a shows the 25 m depth target to be outside the beam pattern at 100 m range and inside the beam pattern at the other ranges. This is reflected in the range dependence of the *SE*. The impact of the increasing average transmission loss on the *SE* with range is seen as a movement of the *SE* distribution patterns to smaller average values with increasing range. It is clear that the histograms or probability distribution for detecting the target changes with range.

The percentage of the projected signals that resulted in a *SE* greater than zero dB for each target depth and range versus changing *FOM* is listed in Table 1. The results are for the 1.38 hour simulation time interval. For instance, the number of detections for a 25 m deep target was 1, 98.5, 91.5, and 98 % for the 100, 200, 400, and 800 m ranges, respectively. If the signal source level is decreased in 20 dB steps to minimize counter detection, the percentage of detections for the 25 m deep target with range decreased as the number of detections with *SE* greater than 0 decreased as shown in Table 1. For a 60 dB decrease in source level, the number of detections became 1, 97.5, 57.5, and 20.5 % for the 100, 200, 400, and 800 m ranges, respectively. The mine hunting sonar performance was compromised as its performance effectiveness was changed due to the internal wave induce variability of the *SE*.

Inter-comparison of *SE* variability for the in water targets at depth 35, 45, and 60 m; Figs. 7–11 show similar characteristics in the *SE* variability as that noted for the target at 25 m. The histograms, i.e., probability distributions of the *SE*, as a function of target depth and range were all different. In general, they were spread over a greater *SE* span of values with increasing range ranging from ~ 20 dB at short ranges to greater than 60 dB at the longer ranges. As noted in Table 1, the performance of the system for each of the target depths was degraded due to the internal wave perturbation of the sound speed field and the *SE*.

Table 1 – Percentage of detections with signal excess (*SE*) greater than 0 dB. The first column lists the depth and range of the target from the mine hunting sonar transducer, i.e., TLM25100 stands for target depth of 25 m target range of 100 m. Source depth was 50 m.

	% SE > 0	% SE > 0	% SE > 0	% SE > 0
FOM	174	154	134	114
TLM25100	1	1	1	1
TLM25200	98.5	98.5	98.5	97.5
TLM25400	91.5	91.5	86.5	57.5
TLM25800	98	96	84.5	20.5
TLM35100	99.5	99.5	99.5	99.5
TLM35200	99.5	99.5	99.5	86
TLM35400	81	79.5	66	34.5
TLM35800	99.5	96.5	85.5	35
TLM45100	100	100	100	99.5
TLM45200	100	100	100	88
TLM45400	94	94	88.5	63.5
TLM45800	100	99.5	94.5	62.5
TLM60100	9	9	8.5	8.5
TLM60200	100	100	100	99.5
TLM60400	100	100	100	90.5
TLM60800	100	99.5	93.5	61
TLM70100	0	0	0	0
TLM70200	35.5	34	23	11.5
TLM70400	100	99.5	98.5	82.5
TLM70800	100	98.5	95	57.5

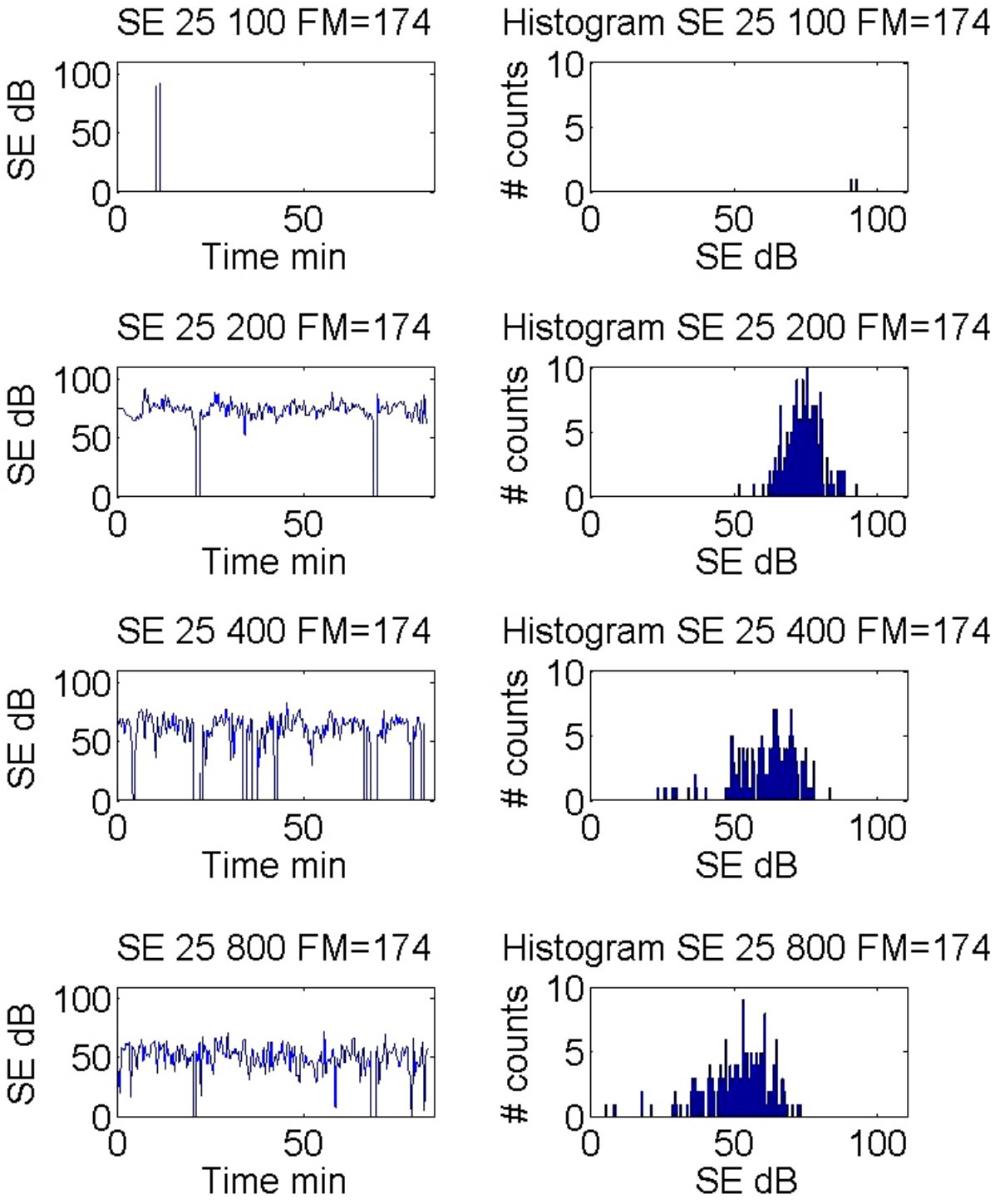

Fig. 7 – Left Column: Signal Excess (*SE*) for a target at 25 m depth and source at 50 m depth for 100 m, 200 m, 400 m, and 800 m ranges. Right column histogram of *SE* for the same ranges. FM is the Figure of Merit.

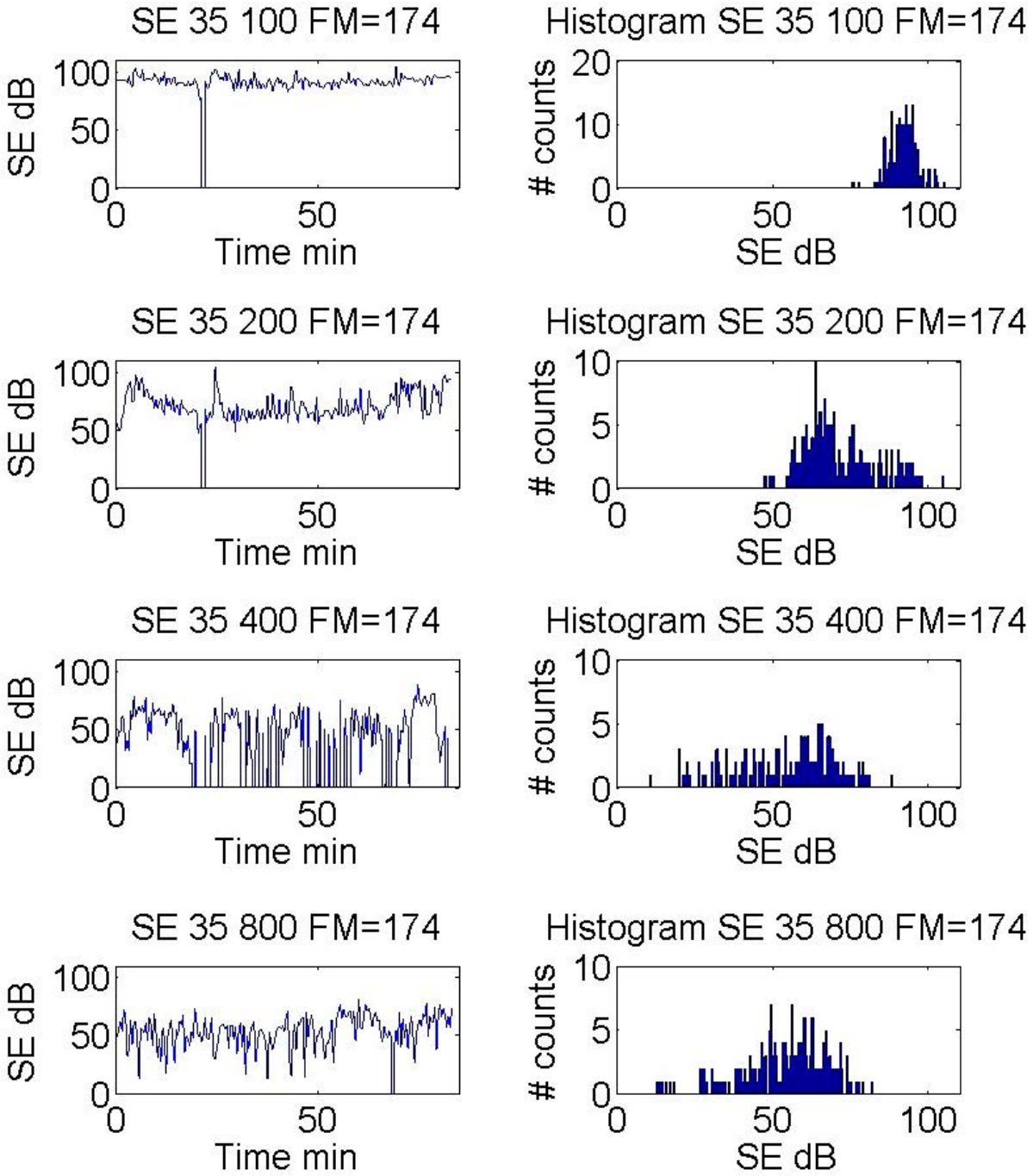

Fig. 8 – Left Column: Signal Excess (*SE*) for a target at 35 m depth and source at 50 m depth for 100 m, 200 m, 400 m, and 800 m ranges. Right column histogram of *SE* for the same ranges. FM is the Figure of Merit.

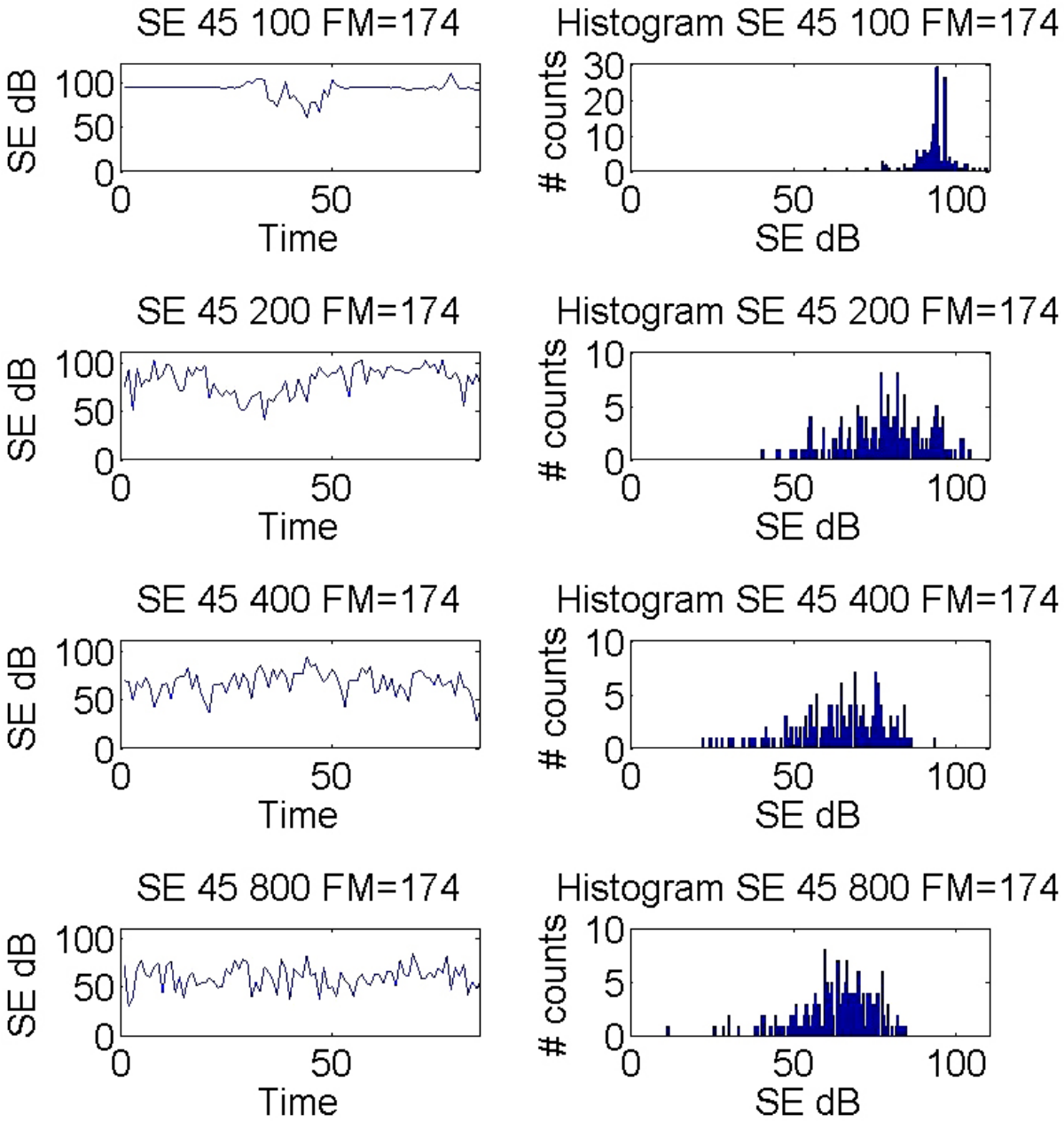

Fig. 9 – Left Column: Signal Excess (*SE*) for a target at 45 m depth and source at 50 m depth for 100 m, 200 m, 400 m, and 800 m ranges. Right column histogram of *SE* for the same ranges. FM is the Figure of Merit.

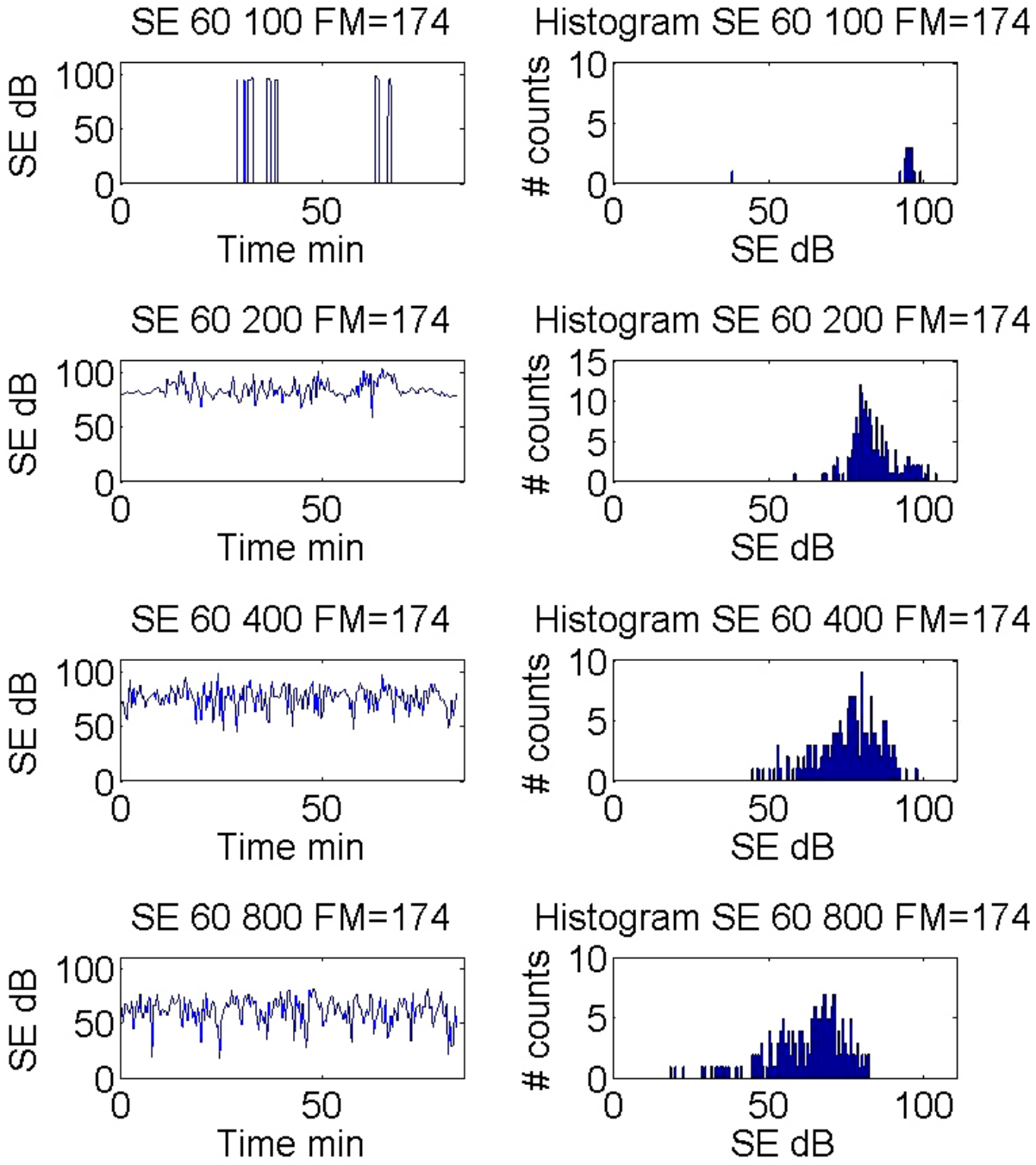

Fig. 10 – Left Column: Signal Excess (*SE*) for a target at 60 m depth and source at 50 m depth for 100 m, 200 m, 400 m, and 800 m ranges. Right column histogram of *SE* for the same ranges. FM is the Figure of Merit.

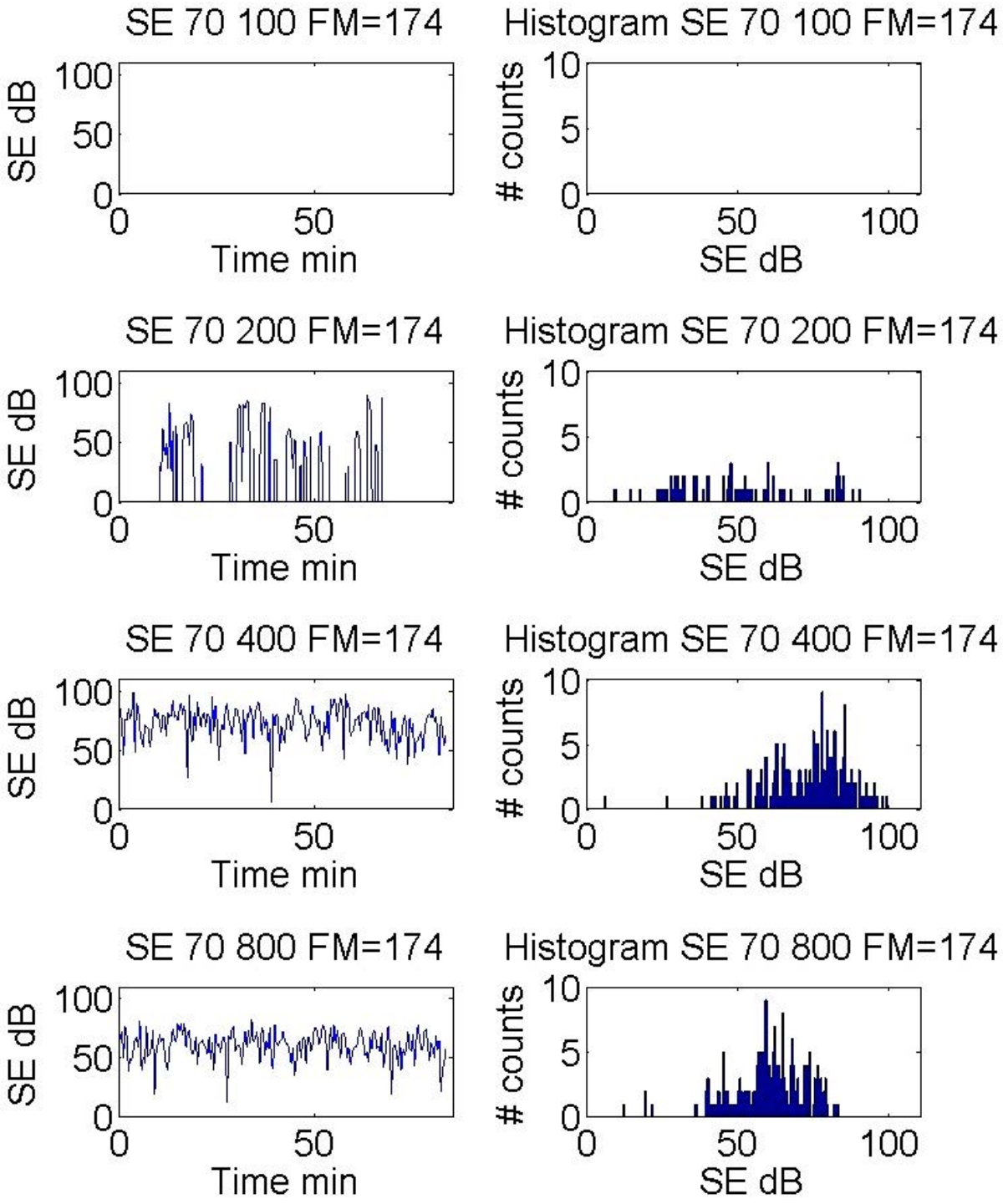

Fig. 11 – Left Column: Signal Excess (*SE*) for a target at 70 m depth and source at 50 m depth for 100 m, 200 m, 400 m, and 800 m ranges. Right column histogram of *SE* for the same ranges. FM is the Figure of Merit.

VI. CONCLUSION

A hypothetical mine detection sonar system's signal excess variability, which was caused by mode 1 internal wave perturbation of the sound speed profile, was calculated for a limited sound speed field time section. Acoustic signals were projected parallel to the propagation direction of the internal wave field. For a sonar system figure of merit equal to 174 dB and at a source depth of 50 m, the histograms of the signal excess variability showed the probability distribution of the system response to be target depth and range dependent. The signal excess variability was distributed over 20 dB for short range targets (~200 m) and by more than 60 dB for longer range targets (400 and 800 m), i.e., signal excess histograms showed increased variability with increasing target range. Within the bounds of the calculation, a system operating at 20 kHz and using a projector with a source level of 240 dB re 1 μPa @ 1 m detected targets with a high percent of its pings; see Table 1 in the FOM = 174 column. This was true if the target was in the transducer's primary beam pattern.

However, if the source level of the sonar system was decreased, e.g., to reduce counter detection, the signal excess variability caused by the internal waves resulted in a significant reduction in the percent of target detections; see Table 1 in the columns labeled FOM = 154 to 114 dB. The degradation in the hypothetical system performance was large enough to call into question its use as a reliable mine detection system when operated at reduced source levels in a sound speed field perturbed by mode 1 internal waves.

VII. REFERENCES

1. M.H. Orr and P.C. Mignerey, "Nonlinear Internal Waves in the South China Sea: Observation of the Conversion of Depression Internal Waves to Elevation Internal Wave", J. Geophys. Res. **108**, 108-123 (2003)

2. R.E. Keenan, "An Introduction to GRAB Eigenrays and CASS Reverberation and Signal Excess," in *Proceedings OCEANS 2000 MTS/IEEE Conference and Exhibition,* 11-14 Sep. 2000, Providence, RI, Vol. 2, pp. 1065 -1070.

3. C. Godoy, R.E. Keenan, and H. Weinberg, *Express Software Test Description and Introductory User's Guide CASS: Comprehensive Acoustic System Simulation*, (Naval Oceanographic Office, Systems Integration Department, Stennis Space Center, MS, 2011), version 4.3, p. 6.

4. Google Earth, https://earth.google.com/

5. S.M. Simpson, M.H. Orr, and E. Tucholski, "(U) Hypothetical Mine Hunting Sonar – Internal Wave Impact on Performance," MR/7100--14-9578, NRL, Washington, DC, October 2014 (Unclassified).

Lieutenant Junior Grade (LTJG) Stewart M. Simpson graduated from the United States Naval Academy in 2013 receiving a B.S. in Physics, with a focus in Acoustics, and a Commission in the United States Navy. His senior project evaluated the impact of a range-dependent, time-dependent, sound velocity profile (SVP) on the performance of a submerged sonar system hunting for targets at various depths and ranges. After graduating from Nuclear Power School in 2013, LTJG Simpson completed Submarine Officer Basic Course (SOBC). While waiting to proceed in the nuclear training pipeline, he assisted in the management of several large contracts for Site Facilities Engineering at the Knolls Atomic Power Laboratory. He then qualified as a nuclear operator in 2015 from Naval Nuclear Power Training Unit (NPTU) Ballston Spa. Currently, he is working with Navy Submarine Medical Research Lab on next generation weapons systems operations and integration, as well as some human performance modeling.

Marshall H. Orr is an Affiliated Full Professor at the University of Delaware's College of Earth, Ocean and Environment. Dr. Orr's research has focused on the impact of ocean fluid processes on the sound speed field and the acoustic signals which propagate through it. Except for a three-year hiatus, he worked in the Acoustics Division of the Naval Research Laboratory from 1992 to 2014 as a Branch Head, Research Scientist, and Associate Superintendent. From 2005 to 2008 he worked in the Chief of Naval Operations Submarine Warfare SSBN Security Technology Program. He was the Ocean Acoustics program manager at the Office of Naval Research Program from 1987 to 1992 and worked in hydrocarbon exploration industry as a research or senior geophysicist from 1981 to 1987. His research program at the Woods Hole Oceanographic Institution from 1974 to 1981 focused on the use of high frequency acoustic signals to image small scale fluid process and sediment transport. Dr. Orr received a Ph.D. in Physics from The Pennsylvania State University in low energy nuclear structure physics in 1972, an M.S. in Physics from the University of Maine in 1967, and a B.S. in Physics from the University of Rhode Island in 1965.

Commander Edward J. Tucholski is a Permanent Military Professor in the Physics Department at the U.S. Naval Academy. Prior to Dr. Tucholski's teaching assignment, he was a submarine warfare officer serving onboard USS *LEWIS AND CLARK* (SSBN 644G) as an Engineering Division Officer, USS *ALEXANDRIA* (SSN 757) as Operations Officer, and USS *DALLAS* (SSN 700) as Executive Officer. He received an M.S. degree in Materials Science and Engineering from The Johns Hopkins University in 1988. His thesis studied propagation of ultrasonic waves in cubic single crystals for the purpose of nondestructive evaluation. He completed a Ph.D. in Physics in 2001 at the Naval Postgraduate School. His research was in physical acoustics, specifically studying the forces on resonant objects due to frequency banded noise fields. Since then he has studied nondestructive analysis of insulation resistance, acoustic emission as a precursor to dielectric failure in the presence of large electric fields, the effect of pressure loading and drive voltage on cymbal transducer impedance changes, as well as various pedagogical projects for education in acoustics. Dr. Tucholski's teaching portfolio includes Physical Acoustics, Underwater Acoustics and Sonar, Advanced Electricity and Magnetism, Introductory Electricity and Magnetism, and calculus-based General Physics I and II.

Table of Contents